

УДК 517.977 + 519.63

MODELING OSMOTIC DE- AND REHYDRATION OF LIVING CELLS USING HAMILTON—JACOBI EQUATIONS AND REACHABLE SET TECHNIQUES¹**V. L. Turova**

The paper describes mathematical models of the osmotic shrinkage and swelling of living cells during freezing and thawing. The cell shape is searched as the level set of a function which satisfies a Hamilton—Jacobi equation resulting from a Stefan-type condition for the normal velocity of the cell boundary. The Hamilton—Jacobi equation is then solved numerically in two and three dimensions using a monotony preserving finite-difference scheme. A generalized variant of the Stefan condition accounting for tension effects in the cell membrane is also considered, and the corresponding cell shape evolution is computed in two dimensions using a reachable set technique arising from conflict control approach.

Key words: Cryopreservation of cells, osmotic effect, mathematical model, Hamilton—Jacobi equations, finite-difference scheme, reachable set.

1. Introduction

The increased usage of living cells in medical applications stimulates the development of cryopreservation techniques that provide the most effective tool for keeping the viability and functionality of isolated cells. However, cooling and warming can cause dangerous cell changes such as excessive shrinkage and swelling due to the osmotic dehydration and rehydration occurring during the freezing and warming phases, respectively. The paper deals with the mathematical modeling of cell shrinkage and swelling caused by the osmotic pressure arising due to different salt concentrations in the extracellular and intracellular liquids.

The existing models of cell dehydration during freezing (see e.g. [1, 6]) describe the change of the cell volume depending on mass diffusion, heat transfer, and the evolution of the freezing front. The cell shape is supposed to be spherical or cylindrical. However, as it is reported by biologists (see e.g. [3]), keeping both the cell size and shape is very important for the cell survival.

Mathematical models proposed in this paper are concerned with the evolution of the cell shape depending on the temperature distribution and the amount of the frozen liquid outside the cell. The models are based on the theory of ice formation in porous media developed in [4] and Stefan type models [2] describing the osmotic outflow (inflow) caused by the increase (decrease) of salt concentration in the extracellular liquid during its freezing (thawing). The resulting model equations of the Hamilton—Jacobi type are treated numerically using both a finite-difference scheme for finding viscosity solutions and the computation of reachable sets of an associated conflict control problem formalized according to [7, 8]. The computed shape evolutions are presented.

2. Mathematical models

Each biological tissue cell is located inside a pore filled with a saline solution called extracellular fluid. The cell interior is separated from the pore by a cell membrane whose structure ensures a very low heat conductivity but a very good permeability for water, which makes possible its easy inflow

¹The work is supported by the German Research Society (DFG), Project SPP 1253. The paper includes joint results with N.D. Botkin

and outflow so that the osmotic pressure caused by the difference of salt concentrations inside and outside the cell easily results in water transport into/out of the cell.

2.1. Dehydration of cells

In the freezing phase, the mechanism of the osmotic effect is the following. Ice formation goes initially in the extracellular solution. Since ice is practically free of salt, the water to ice phase transition results in the increase of salt concentration (c_{out}) in the remaining extracellular liquid. The osmotic pressure forces the outflow of water from the cell to balance the intracellular (c_{in}) and extracellular salt concentrations. Modeling the cell shrinkage is based on free boundary problem techniques. The main relation here is the so called Stefan condition: $V_n = \alpha(c_{\text{out}} - c_{\text{in}})$, where V_n is the normal velocity of the cell boundary (directed to the cell interior), and the right-hand-side represents the osmotic flux that is proportional to the difference of the concentrations. Extracellular salt concentration c_{out} depends on the unfrozen fraction β_ℓ of the extracellular liquid. The function β_ℓ is governed by the following phase field model [4]:

$$\rho C \frac{\partial \theta}{\partial t} + \rho L \frac{\partial \beta_\ell}{\partial t} - \mathcal{K} \Delta \theta = 0, \quad \beta_\ell = \phi \left(\frac{L\theta}{T_0(T_0 + \theta)} \right), \quad (2.1)$$

where θ is the Celsius temperature, $T_0 \approx 273^\circ\text{K}$ the freezing point, L the latent heat, ρ the density, C the specific heat capacity, \mathcal{K} the heat conductivity coefficient. The function ϕ is recovered from experimental data. Note that β_ℓ as a function of the temperature is a constitutive material law that, e.g. in frozen-soil science, is measured directly by nuclear magnetic resonance.

The intracellular and extracellular salt concentrations are estimated using the mass conservation law as follows:

$$c_{\text{in}} = c_{\text{in}}^0 W_c^0 / W_c, \quad c_{\text{out}} = c_{\text{out}}^0 W^0 / W,$$

where W_c^0 and W_c are, respectively, the initial and current cell volumes, W^0 and W are the initial and current volumes of the unfrozen part of the pore. The current volume W at the time t is computed as

$$W(t) = \int_{W^0} \beta_\ell(\theta(t, x)) dx,$$

where $\theta(t, x)$ is found using finite element approximation of the phase field model (2.1). A typical form of the function $W(t)$ is shown in Fig. 1.

The cell region $\Sigma(t)$ is searched as the level set of a function $\Psi(t, x)$:

$$\Sigma(t) = \{x: \Psi(t, x) \leq 1\}, \quad x \in \mathbb{R}^3 \text{ (or } \mathbb{R}^2).$$

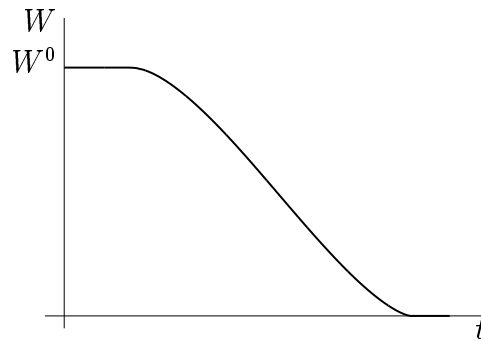


Fig 1. Evolution of the volume of the unfrozen extracellular liquid versus time.

Assuming that the cell boundary propagates with the normal velocity V_n yields the following Hamilton—Jacobi equation for the function $\Psi(t, x)$:

$$\Psi_t - \alpha(c_{\text{out}} - c_{\text{in}})|\nabla\Psi| = 0 \quad (2.2)$$

with $\Psi(0, x) = \inf\{\lambda > 0: x \in \lambda \cdot \Sigma(0)\}$. Here $|\nabla\Psi|$ denotes the Euclidean norm of the gradient.

2.2. Rehydration of cells

In the thawing phase, the osmotic effect results in the cell inflow and hence in cell swelling. We use the following mass conservation law for the salt content:

$$W_c^0 c_{\text{in}}^0 = W_s c_{\text{in}}^0 + W_\ell c_{\text{in}}, \quad W_c = W_s + W_\ell, \quad (2.3)$$

where W_c^0 is the initial volume of the frozen cell; W_c is the current volume of the cell; W_s and W_ℓ are volumes of the frozen and unfrozen parts of the cell, respectively; c_{in}^0 and c_{in} are the salt concentrations in the frozen and unfrozen parts of the cell, respectively. From (2.3), one obtains

$$c_{\text{in}} = c_{\text{in}}^0 \left(1 + (W_c^0 - W_c)/W_\ell\right).$$

We assume that

$$W_\ell(t) \approx \int_{W_c^0} \beta_\ell(\theta(t, x)) dx,$$

where the function β_ℓ shows now the volume fraction of unfrozen intracellular fluid. The salt concentration c_{out} outside the cell is supposed to be constant.

Admitting that the propagation velocity V_n of the cell boundary is proportional to the difference of the concentrations c_{in} and c_{out} , one arrives at the equation of the form (2.2).

3. Finite-difference scheme for solving Hamilton—Jacobi equation

Hamilton—Jacobi equation (2.2) is solved numerically using a finite difference scheme for finding viscosity solutions. This section describes a proper scheme. Conventionally, the symbol $|h|$ denotes the absolute value of h in the case of scalar or the Euclidian norm of h in the case of vector.

Consider a general form of the Hamilton—Jacobi equation but assume for simplicity that the spatial variable is three dimensional:

$$\Psi_t + H(t, x, \Psi_x) = 0, \quad \Psi(0, x) = \sigma(x). \quad (3.1)$$

Here $x = (x_1, x_2, x_3) \in \mathbb{R}^3$; $t \in [0, \infty)$; $\Psi: [0, \infty) \times \mathbb{R}^3 \rightarrow \mathbb{R}$; and $\sigma: \mathbb{R}^3 \rightarrow \mathbb{R}$ is some given function. Assume that the Hamiltonian H is defined as

$$H(t, x, p) = \max_{v \in Q} \min_{u \in P} \langle p, f(t, x, u, v) \rangle,$$

where f is the right-hand side of the following conflict controlled system

$$\dot{x} = f(t, x, u, v), \quad x \in \mathbb{R}^3, \quad u \in P \subset \mathbb{R}^p, \quad v \in Q \subset \mathbb{R}^q, \quad p, q \leq 3. \quad (3.2)$$

The function f is assumed to be uniformly continuous on $[0, \infty) \times \mathbb{R}^3 \times P \times Q$, bounded and Lipschitz-continuous in t, x , the function σ being bounded and Lipschitz-continuous in x .

Let $\tau, \Delta_{x_i}, i = 1, 2, 3$, are time and space discretization steps. Introduce the following notation:

$$\Psi^n(x_1^i, x_2^j, x_3^k) = \Psi(t_n, i\Delta_{x_1}, j\Delta_{x_2}, k\Delta_{x_3}), \quad t_n = n\tau$$

and consider a difference scheme:

$$\Psi^{n+1}(x_1^i, x_2^j, x_3^k) = \Psi^n(x_1^i, x_2^j, x_3^k) - \tau H(t_n, x_1^i, x_2^j, x_3^k, \Psi_{x_1}^n, \Psi_{x_2}^n, \Psi_{x_3}^n), \quad \Psi^0(x_1^i, x_2^j, x_3^k) = \sigma(x_1^i, x_2^j, x_3^k).$$

Here, the symbols $\Psi_{x_1}^n, \Psi_{x_2}^n, \Psi_{x_3}^n$ denote finite difference approximations (left, right, central and etc.) of the corresponding partial derivatives.

The scheme can be considered as the successive application of an operator Π to the grid functions:

$$\Psi^{n+1} = \Pi(\Psi^n; t_n, \tau, \Delta_{x_1}, \Delta_{x_2}, \Delta_{x_3}).$$

Note that such an operator can be naturally extended to continuum functions.

Definition 1. The operator Π is monotone, if the following implication holds:

$$\Psi \leq \Phi \Rightarrow \Pi(\Psi; t, \tau, \Delta_{x_1}, \Delta_{x_2}, \Delta_{x_3}) \leq \Pi(\Phi; t, \tau, \Delta_{x_1}, \Delta_{x_2}, \Delta_{x_3}),$$

where the point-wise order is assumed.

Definition 2. The operator Π has the generator property, if the following holds:

$$\left| \frac{\Pi(\phi; t, \tau, a_1\tau, a_2\tau, a_3\tau)(x) - \phi(x)}{\tau} + H(t, x, D\phi(x)) \right| \leq C(1 + \|D\phi\| + \|D^2\phi\|)\tau$$

for every $\phi \in C_b^2(\mathbb{R}^3)$, $x = (x_1, x_2, x_3) \in \mathbb{R}^3$, and fixed $a_1, a_2, a_3 > 0$. Here $C_b^2(\mathbb{R}^3)$ is the space of twice continuously differentiable functions defined on \mathbb{R}^3 and bounded together with their two derivatives, $\|\cdot\|$ denotes the point-wise maximum norm, $D\phi$ and $D^2\phi$ denote the gradient and the Hessian matrix of ϕ .

Theorem 1 (convergence, [10]). *Assume that the operator $\Pi(\cdot; t, \tau, a_1\tau, a_2\tau, a_3\tau)$ is monotone for any $t, \tau > 0$ and satisfies the generator property, then the grid function obtained by the procedure:*

$$\Psi^{n+1} = \Pi(\Psi^n; t_n, \tau, a_1\tau, a_2\tau, a_3\tau), \quad n = 0, 1, \dots, \quad \Psi^0 = \sigma,$$

converges point-wise to a viscosity solution of Hamilton—Jacobi equation (3.1) as $\tau \rightarrow 0$, and the convergence rate is $\sqrt{\tau}$.

Let us describe a finite difference scheme which fulfils the conditions of Theorem 1. The scheme is based on the operator introduced in [5]. The main idea is to use either the right or the left divided differences for the approximation of the spatial derivatives Ψ_{x_m} , $m = 1, 2, 3$, depending on the sign of f_m , where f_m is the m -th component of the right hand side of system (3.2).

Denote

$$\begin{aligned} p_1^R &= [\Psi^n(x_1^{i+1}, x_2^j, x_3^k) - \Psi^n(x_1^i, x_2^j, x_3^k)]/\Delta_{x_1}, & p_1^L &= [\Psi^n(x_1^i, x_2^j, x_3^k) - \Psi^n(x_1^{i-1}, x_2^j, x_3^k)]/\Delta_{x_1}, \\ p_2^R &= [\Psi^n(x_1^i, x_2^{j+1}, x_3^k) - \Psi^n(x_1^i, x_2^j, x_3^k)]/\Delta_{x_2}, & p_2^L &= [\Psi^n(x_1^i, x_2^j, x_3^k) - \Psi^n(x_1^i, x_2^{j-1}, x_3^k)]/\Delta_{x_2}, \\ p_3^R &= [\Psi^n(x_1^i, x_2^j, x_3^{k+1}) - \Psi^n(x_1^i, x_2^j, x_3^k)]/\Delta_{x_3}, & p_3^L &= [\Psi^n(x_1^i, x_2^j, x_3^k) - \Psi^n(x_1^i, x_2^j, x_3^{k-1})]/\Delta_{x_3}, \\ & & a^+ &= \max(a, 0), \quad a^- = \min(a, 0). \end{aligned}$$

In [5], the following approximation of the spatial derivatives is suggested:

$$\Psi_{x_1}^n \cdot f_1 = p_1^L \cdot f_1^+ + p_1^R \cdot f_1^-, \quad \Psi_{x_2}^n \cdot f_2 = p_2^L \cdot f_2^+ + p_2^R \cdot f_2^-, \quad \Psi_{x_3}^n \cdot f_3 = p_3^L \cdot f_3^+ + p_3^R \cdot f_3^-,$$

where f_1, f_2, f_3 are the right-hand-sides of system (3.2) computed at $(t_n, x_1^i, x_2^j, x_3^k, u, v)$; p_1^R, p_2^R, p_3^R and p_1^L, p_2^L, p_3^L the right and the left divided differences, respectively. Thus, the operator is given by

$$\Pi(\Psi^n; t_n, \tau, \Delta_{x_1}, \Delta_{x_2}, \Delta_{x_3})(x_1^i, x_2^j, x_3^k) = \Psi^n(x_1^i, x_2^j, x_3^k) - \tau \max_{v \in Q} \min_{u \in P} \sum_{m=1}^3 (p_m^L \cdot f_m^+ + p_m^R \cdot f_m^-). \tag{3.3}$$

Here, the arguments $t_n, x_1^i, x_2^j, x_3^k, u, v$ of f_m^- and f_m^+ are omitted for brevity.

Let us prove that the operator Π meets the requirements of Theorem 1. The following lemmas hold.

Lemma 1 (monotonicity). *Let M be the bound of $|f|$. If $a_1, a_2, a_3 \geq M\sqrt{3}$, then the operator $\Pi(\cdot; t, \tau, a\tau, b\tau, c\tau)$ given by (3.3) is monotone.*

P r o o f. Suppose $\Psi \leq \Phi$. Let us show that $\Pi(\Psi; t, \tau, a_1\tau, a_2\tau, a_3\tau) \leq \Pi(\Phi; t, \tau, a_1\tau, a_2\tau, a_3\tau)$. Denote $\mathfrak{h}_1 = (a_1, 0, 0)$, $\mathfrak{h}_2 = (0, a_2, 0)$, $\mathfrak{h}_3 = (0, 0, a_3)$. We have

$$\begin{aligned} & \Pi(\Psi; t, \tau, a_1\tau, a_2\tau, a_3\tau)(x) - \Pi(\Phi; t, \tau, a_1\tau, a_2\tau, a_3\tau)(x) = \Psi(x) - \Phi(x) \\ & - \tau \max_{v \in Q} \min_{u \in P} \sum_{m=1}^3 \left(\frac{\Psi(x) - \Psi(x - \mathfrak{h}_m\tau)}{a_m\tau} f_m^+ + \frac{\Psi(x + \mathfrak{h}_m\tau) - \Psi(x)}{a_m\tau} f_m^- \right) \\ & + \tau \max_{v \in Q} \min_{u \in P} \sum_{m=1}^3 \left(\frac{\Phi(x) - \Phi(x - \mathfrak{h}_m\tau)}{a_m\tau} f_m^+ + \frac{\Phi(x + \mathfrak{h}_m\tau) - \Phi(x)}{a_m\tau} f_m^- \right). \end{aligned}$$

By rearranging terms and using the obvious relations $f_m^+ - f_m^- = |f_m|$ and $\max_v \min_u g_1(u, v) - \max_v \min_u g_2(u, v) \leq \max_v \max_u [g_1(u, v) - g_2(u, v)]$, one obtains

$$\begin{aligned} & \Pi(\Psi; t, \tau, a_1\tau, a_2\tau, a_3\tau)(x) - \Pi(\Phi; t, \tau, a_1\tau, a_2\tau, a_3\tau)(x) \leq \Psi(x) - \Phi(x) \\ & + \tau \max_{v \in Q} \max_{u \in P} \sum_{m=1}^3 \left[\left(\frac{\Psi(x - \mathfrak{h}_m\tau) - \Phi(x - \mathfrak{h}_m\tau)}{a_m\tau} - \frac{\Psi(x) - \Phi(x)}{a_m\tau} \right) f_m^+ \right. \\ & \left. + \left(\frac{\Psi(x + \mathfrak{h}_m\tau) - \Phi(x + \mathfrak{h}_m\tau)}{a_m\tau} - \frac{\Psi(x) - \Phi(x)}{a_m\tau} \right) (-f_m^-) \right] \\ & \leq \Psi(x) - \Phi(x) - \tau \sum_{m=1}^3 \frac{|f_m|}{a_m\tau} (\Psi(x) - \Phi(x)) = \left(1 - \sum_{m=1}^3 \frac{|f_m|}{a_m} \right) (\Psi(x) - \Phi(x)). \end{aligned}$$

With $\sum_{m=1}^3 |f_m| \leq \sqrt{3}M$ one comes to $1 - \sum_{m=1}^3 \frac{|f_m|}{a_m} > 0$, which finally implies the required inequality.

Lemma 2 (generator property). *The generator property holds for the operator Π .*

P r o o f. Let $\phi \in C_b^2(\mathbb{R}^3)$. Denote $\mathfrak{d}_1 = (\Delta_{x_1}, 0, 0)$, $\mathfrak{d}_2 = (0, \Delta_{x_2}, 0)$, $\mathfrak{d}_3 = (0, 0, \Delta_{x_3})$. We have

$$\Pi(\phi; t, \tau, \Delta_{x_1}, \Delta_{x_2}, \Delta_{x_3})(x) = \phi(x) - \tau \max_{v \in Q} \min_{u \in P} \sum_{m=1}^3 \left(\frac{\phi(x) - \phi(x - \mathfrak{d}_m)}{\Delta_{x_m}} f_m^+ + \frac{\phi(x + \mathfrak{d}_m) - \phi(x)}{\Delta_{x_m}} f_m^- \right).$$

Estimate

$$\begin{aligned} & \left| \frac{\Pi(\phi; t, \tau, \Delta_{x_1}, \Delta_{x_2}, \Delta_{x_3})(x) - \phi(x)}{\tau} + \max_{v \in Q} \min_{u \in P} \langle D\phi(x), f \rangle \right| \\ & = \left| - \max_{v \in Q} \min_{u \in P} \sum_{m=1}^3 \left(\frac{\phi(x) - \phi(x - \mathfrak{d}_m)}{\Delta_{x_m}} f_m^+ + \frac{\phi(x + \mathfrak{d}_m) - \phi(x)}{\Delta_{x_m}} f_m^- \right) + \max_{v \in Q} \min_{u \in P} \sum_{m=1}^3 \frac{\partial \phi}{\partial x_m} (f_m^+ + f_m^-) \right| \\ & \leq \max_{u \in P} \max_{v \in Q} \sum_{m=1}^3 \left| \left(\frac{\partial \phi}{\partial x_m} - \frac{\phi(x) - \phi(x - \mathfrak{d}_m)}{\Delta_{x_m}} \right) f_m^+ + \left(\frac{\partial \phi}{\partial x_m} - \frac{\phi(x + \mathfrak{d}_m) - \phi(x)}{\Delta_{x_m}} \right) f_m^- \right| \\ & \leq M \|D^2\phi\| \sum_{m=1}^3 \Delta_{x_m}. \end{aligned}$$

Here M is the bound of $|f|$. Choosing $\Delta_{x_m} = a_m\tau$ and letting $C = \sum_{m=1}^3 a_m$ yields

$$\left| \frac{\Pi(\phi; t, \tau, \Delta_{x_1}, \Delta_{x_2}, \Delta_{x_3})(x) - \phi(x)}{\tau} + H(t, x, D\phi(x)) \right| \leq M C \|D^2\phi\| \tau.$$

4. Three dimensional simulation of cell shrinkage

The finite difference scheme based on the operator Π is implemented as a parallelized program on a Linux cluster. We compute the evolution of the cell boundary during freezing. The function f in our case is

$$f(t, u, v) = \alpha(c_{\text{out}}(t) - c_{\text{in}}(t))^+ u + \alpha(c_{\text{out}}(t) - c_{\text{in}}(t))^- v, \quad u, v \in \mathbb{R}^3, \quad |u| \leq 1, \quad |v| \leq 1.$$

The spatial grid $200 \times 200 \times 200$ for the cubic region $0.3 \times 0.3 \times 0.3$ was utilized, and 1000 time steps of the size $\tau = 0.001$ were done. The run time is about 26 minutes on 30 threads. The initial shape is presented in Fig. 2a. Figures 2b and 2c show the computed shape at the time instants $t = 0.8$ and $t = 0.92$.

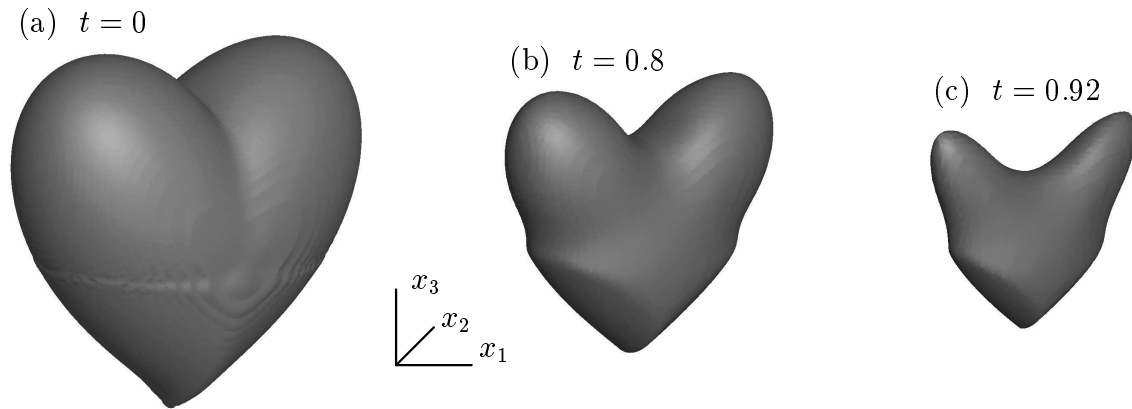


Fig 2. Osmotic cell shrinkage during freezing.

5. Accounting for the membrane tension using reachable set approach

In reality, the deformation of the cell membrane depends on the membrane tension which is a function of the curvature. Therefore, a more realistic expression for the normal velocity of the cell boundary would be:

$$V_n(t, x) = \alpha(c_{\text{out}}(t) - c_{\text{in}}(t)) + \gamma\sigma(x),$$

where $\sigma(x)$ is the angular curvature at the current point x of the cell boundary, and γ is a constant. The angular curvature is explained in Fig. 3. The corresponding Hamiltonian is

$$H(t, x, p) = -(\alpha(c_{\text{out}}(t) - c_{\text{in}}(t)) + \gamma\sigma(x))|p|. \quad (5.1)$$

Note that accounting for the curvature can alter the convexity/concavity structure of the Hamiltonian depending on the state x .

Instead of finding viscosity solutions to equation (3.1), the value function of an appropriate conflict controlled problem with the Hamiltonian (5.1) will be computed. We will treat this problem within the framework of [7, 8, 11]. The consideration will be carried out in \mathbb{R}^2 .

It is easy to see that the conflict controlled system of the form

$$\dot{x} = \alpha(c_{\text{out}}(t) - c_{\text{in}}(t) + \gamma\sigma(x))^+ u + \alpha(c_{\text{out}}(t) - c_{\text{in}}(t) + \gamma\sigma(x))^- v; \quad x, u, v \in \mathbb{R}^2, \quad |u| \leq 1, \quad |v| \leq 1 \quad (5.2)$$

has the Hamiltonian (5.1). The initial cell shape $\Sigma_0 = \Sigma(0)$ is considered as a target set of the differential game where the control u strives to bring the state vector of (5.2) to Σ_0 , and the objective of the control v is opposite.

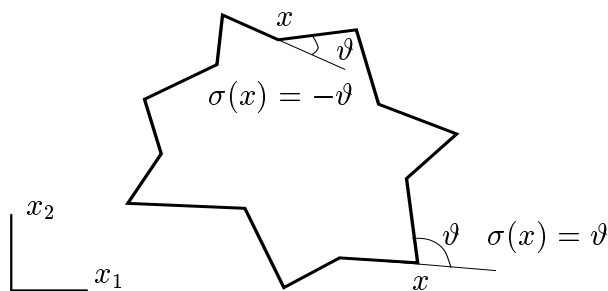


Fig 3. Explanation of the angular curvature.

Since only one control is active at every time t and every point x (the control u acts, if $V_n > 0$; otherwise the control v), one can reduce the construction of level sets of the value function of system (5.2) to finding reachable sets of the controlled system

$$\dot{x} = \text{sign } V_n \cdot u; \quad x, u \in \mathbb{R}^2, \quad u \in |V_n| S, \quad S = \{x \in \mathbb{R}^2 : |x| \leq 1\} \quad (5.3)$$

with Σ_0 being the initial set.

Denote by $x(t; x_0, u(\cdot))$ the state vector of system (5.3) at time $t \geq 0$ provided that x_0 is the initial point at time $t = 0$ and $u(\cdot)$ is an admissible measurable control acting on the time interval $[0, t]$. The set of points reachable from Σ_0 at time t is

$$G(t, \Sigma_0) = \bigcup_{x_0 \in \Sigma_0} \bigcup_{u(\cdot)} x(t; x_0, u(\cdot)).$$

The algorithm for the numerical construction of the sequence $\{\mathcal{G}_i = G(i\Delta t, \mathcal{G}_{i-1}), i = 1, 2, \dots, \mathcal{G}_0 = \Sigma_0\}$, is similar to that one described in [9]. The difference is that the treatment of the cases of local concavity and local convexity alters depending on the sign of V_n .

Simulation results showing the time evolution of the cell shape during freezing are presented in Fig. 4. The sequence of reachable sets is computed on the time interval $[0, 0.645]$ with the time step $\Delta t = 0.001$, every fourth set is drawn. The restriction on the control is $u \in |V_n| P \cdot S$, where $P = \{p_{ij}\}$ is the 2×2 -diagonal matrix introducing anisotropy ($p_{11} = 3, p_{22} = 1$). For the left picture, $\gamma = 0$, i.e. the curvature independent case is considered. For the right picture, $\gamma = 0.06$.

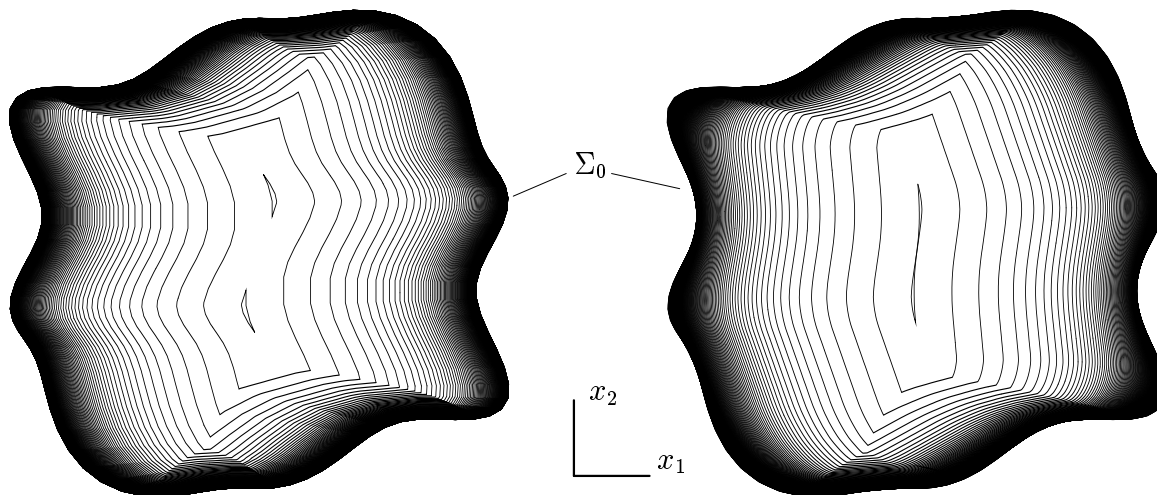


Fig 4. Time evolution of the cell during freezing. To the left: without accounting for the curvature. To the right: with accounting for the curvature.

Note that the low propagation velocity at the beginning of the process results in the accumulation of lines (dark regions) near the initial cell boundary.

In Figure 5, an example of the simulation of cell rehydration during thawing is presented. The computation is done on the time interval $[0, 9.7]$ with the time step $\Delta t = 0.002$. Every 100-th reachable set is drawn. At the finish of the process the stabilization of sets is observed due to the achieved equilibrium of salt concentrations inside and outside the cell.

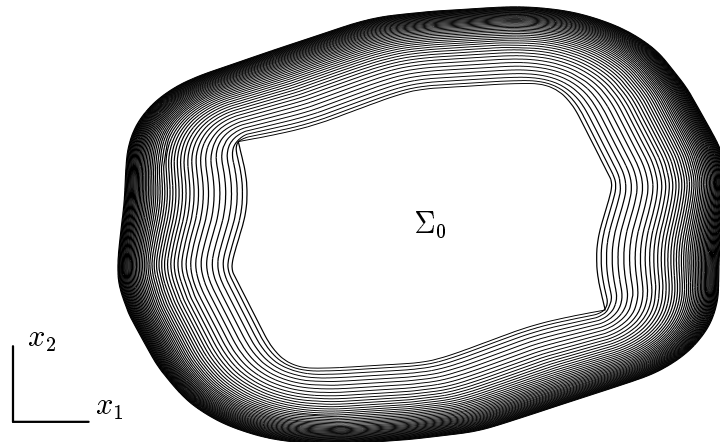


Fig 5. Time evolution of the cell during thawing with accounting for the curvature.

REFERENCES

1. **Batycky R.P., Hammerstedt R., Edwards D.A.** Osmotically driven intracellular transport phenomena // *Phil. Trans. R. Soc. Lond. A.* 1997. Vol. 355. P. 2459–2488.
2. **Caginalp G.** An analysis of a phase field model of a free boundary // *Arch. Rat. Mech. Anal.* 1986. Vol. 92. P. 205–245.
3. **Chen S.C., Mrksich M., Huang S., Whitesides G.M., Ingber D.E.** Geometric control of cell life and death // *Science.* 1997. Vol. 276. P. 1425–1428.
4. **Frémond M.** *Non-Smooth Thermomechanics.* Berlin: Springer, 2002, 480 p.
5. **Malafeyev O.A., Troeva M. S.** A weak solution of Hamilton—Jacobi equation for a differential two-person zero-sum game. // *Preprints of the Eighth International Symposium on Differential Games and Applications, Maastricht, Netherlands, July 5–7, 1998.* P. 366–369.
6. **Mao L., Udaykumar H.S., Karlsson J.O.M.** Simulation of micro scale interaction between ice and biological cells // *Int. J. of Heat and Mass Transfer.* 2003. Vol. 46. P. 5123–5136.
7. **Krasovskii N.N, Subbotin A.I.** *Positional Differential Games.* Moscow: Nauka, 1974. p. (in Russian).
8. **Krasovskii N.N, Subbotin A.I.** *Game-Theoretical Control Problems.* New York; Berlin; Heidelberg: Springer-Verlag, 1988. 517 p.
9. **Patsko V.S., Turova V.L.** From Dubins' car to Reeds and Shepp's mobile robot // *Comput. Visual. Sci.* 2009. Vol. 13, no. 7. P. 345–364.
10. **Souganidis P.E.** Approximation schemes for viscosity solutions of Hamilton—Jacobi equations // *J. of Diff. Eq.* 1985. Vol. 59. P. 1–43.
11. **Subbotin A.I.** *Generalized Solutions of First Order PDEs.* Boston: Birkhäuser, 1995. 312 p.

Turova Varvara Leonidovna
 Cand. of Phys.-Math. Sciences
 Researcher
 Technische Universität München, Germany
 e-mail: turova@ma.tum.de

Received February 12, 2010